



A spatially resolved 39-month dataset of precipitation water isotopes over Jeju volcanic island, Korea

Kwang-Sik Lee¹, Dong-Chan Koh^{2,3}, Young-Hee Kim⁴, Won-Bae Park⁵, Songyi Kim⁴, Hyejung Jung⁴, Yeon-Sik Bong¹, Woo-Jin Shin¹, Chaeyoung Kim⁴, Jeonghoon Lee^{4,*}

5 ¹Center for Earth and Planetary Material Analysis, Korea Basic Science Institute, Ochang, Chungbuk 28119, South Korea

²Korea Institute of Geoscience and Mineral Resources, Daejeon 34132, South Korea

³Geoscience, University of Science and Technology, Daejeon 34113, South Korea

⁴Dept. of Science Education (Earth Science), Ewha Womans University, Seoul 03760, South Korea

⁵The Jeju Institute, Jeju-si, Jeju-do 63147, South Korea

10

Correspondence to: Jeonghoon Lee (jeonghoon.d.lee@gmail.com)

Abstract. Spatially and temporally resolved observations of precipitation water isotopes are essential for quantifying groundwater recharge, constraining hydroclimate variability, and calibrating paleoclimate proxies, yet such datasets remain scarce for monsoon-influenced volcanic islands characterized by steep topography and strong maritime and continental interactions. Here, we present a spatially resolved 39-month dataset (September 2000 to December 2003) of precipitation water isotopes ($\delta^{18}\text{O}$, δD , and d-excess) collected from 15 monitoring stations across Jeju volcanic island, South Korea, spanning elevations from 10 to 1,500 m above sea level. The dataset comprises 462 precipitation samples and captures pronounced seasonal variability together with island-wide spatial gradients. Monthly mean isotope values exhibit a distinct monsoon-driven seasonal cycle, with isotopic depletion during summer and enrichment during winter, which is well represented by sinusoidal fitting for $\delta^{18}\text{O}$ and δD . Spatial analyses reveal a clear altitude effect, with mean lapse rates of -0.15‰ per 100 m for $\delta^{18}\text{O}$ and -1.1‰ per 100 m for δD , while d-excess displays weaker elevation dependence but pronounced seasonal sensitivity to moisture source humidity and evaporation conditions. This dataset provides a robust observational basis for developing high-resolution regional isoscapes, estimating groundwater recharge elevations, and serving as benchmark input and validation data for isotope-enabled climate and hydrological models. All data are openly available with comprehensive metadata, enabling direct reuse in hydrological, climatological, and paleoclimate studies across monsoon-affected volcanic island environments.

15

20

25

1 Introduction

Stable isotope compositions of precipitation ($\delta^{18}\text{O}$, δD , and d-excess) are fundamental tracers for quantifying hydrological processes, identifying groundwater recharge zones, and interpreting atmospheric moisture transport pathways (Dansgaard, 1964; Lee et al., 2010; Dee et al., 2023; Jung et al., 2025). They provide essential baseline information for ecohydrological studies, hydroclimate modeling, and paleoclimate reconstruction, particularly when integrated into isotope-enabled climate models, regional isoscapes, and proxy interpretation frameworks (Feng et al., 2009; Uemura et al., 2012; Konecky et al., 2020). While long-term observations from networks such as the Global Network of Isotopes in Precipitation (GNIP) have

30



improved understanding of temporal isotopic variability, their sparse spatial coverage, mainly limited to urban or low-
altitude locations, restricts their ability to capture elevation-dependent gradients, orographic effects, and moisture source
35 transitions (Posmentier et al., 2004; Peng et al., 2010). Long-term, spatially distributed observations of precipitation isotopes
remain scarce in monsoon-influenced volcanic islands. This limitation is especially critical in volcanic island environments,
where steep topography, maritime influence, and monsoon-driven circulation interact to produce strong spatial isotopic
variability. Consequently, there is a growing need for spatially resolved, multi-site, long-term precipitation isotope datasets
that can support groundwater recharge estimation, local lapse-rate calibration, and development of high-resolution isoscapes
40 (Prada et al., 2016; Kim et al., 2026).

Volcanic islands, in particular, represent highly dynamic hydroclimatic environments where rapid elevation changes,
steep orographic gradients, and interactions between maritime and continental air masses strongly influence the isotopic
compositions of precipitation (Guan et al., 2009; Lee et al., 2013). These complex atmospheric and hydrological conditions
produce significant spatial variability in isotopic fractionation via Rayleigh distillation, sub-cloud evaporation, and seasonal
45 shifts in moisture source regions (Xie et al., 2022). Yet, existing studies on volcanic islands have been restricted to either
event-based measurements or short-term monitoring at isolated stations, resulting in datasets that lack spatial continuity across
elevation, cardinal direction, and coastal-inland gradients (Lee et al., 1999; Koh et al., 2012). Such limitations are particularly
critical when interpreting paleoclimate archives, including speleothems, cave dripwaters, and lacustrine deposits, which require
accurate modern baseline isotopic data to calibrate proxy signals (Woo et al., 2008; Johnson and Ingram, 2004). Without
50 reliable spatiotemporal precipitation isotopic observations, proxy interpretations may misrepresent moisture source variability,
altitude effects, or the seasonality of infiltration, particularly in monsoon-affected volcanic island environments where these
signals are amplified (Peng et al., 2010; Uemura et al., 2012). Establishing a spatially resolved isotopic framework is therefore
essential for paleoclimate reconstruction, groundwater recharge estimation, and hydrogeochemical modeling in such
environments (Wang et al., 2024).

To address these gaps, we present a unique dataset comprising 462 precipitation samples collected over 39 months from
fifteen monitoring stations located across Jeju volcanic island, South Korea. These stations were strategically selected to
capture topographic, climatic, and geographic variability, covering elevation gradients, windward and leeward slopes, and
coastal-to-inland transitions. The dataset includes $\delta^{18}\text{O}$, δD , and d-excess measurements, together with meteorological
parameters, enabling comprehensive evaluation of seasonal and spatial isotopic patterns as well as altitude effects. Extensive
60 quality control procedures, standardized sampling protocols, and VSMOW-referenced laboratory analyses ensure that the
dataset is robust, reproducible, and suitable for integration into regional and global applications (Lee et al., 2003; Yoshimura
et al., 2011). The dataset provides a rare combination of temporal continuity and spatial coverage, making it particularly well
suited for isotope-enabled climate modeling, groundwater recharge estimation, isoscape development, and paleoclimate proxy
calibration in monsoon-influenced volcanic island environments (Koh et al., 2022). By quantifying both seasonal cyclicality and



65 altitudinal gradients, this study offers new insights into how moisture sources, topographic forcing, and atmospheric circulation
jointly regulate precipitation isotope signatures across East Asia. Moreover, the dataset serves as a benchmark resource for
improving isotope-based hydrological models (e.g., IsoGSM, Yoshimura et al., 2011) and for validating paleoclimate
reconstructions in regions with complex orography and climate variability.

2 Study area and method

70 2.1 Geographical and climatic features of Jeju island

Jeju Island is a volcanic oceanic island located approximately 100 km south of the Korean Peninsula, situated in the path of
the East Asian monsoon system. The island covers an area of 1,845 km² and is dominated by Mt. Halla (1,950 m a.s.l.), a
shield volcano representing the highest peak in South Korea. The terrain exhibits a pronounced altitudinal gradient,
transitioning from low-lying coastal plains to mid-elevation basaltic lava fields, and culminating in alpine volcanic terrain near
75 the summit. This steep, radial topography shapes not only precipitation distribution and orographic lifting processes but also
atmospheric cooling trajectories that govern Rayleigh distillation and isotope fractionation. As shown in Figure 1, the central
peak acts as an orographic barrier, producing strong spatial contrasts in precipitation isotope signatures between windward and
leeward slopes. Geologically, Jeju Island consists predominantly of highly fractured basalt, with localized occurrences of
trachyte and pyroclastic deposits. The permeable volcanic substrates facilitate rapid infiltration and minimal surface runoff,
80 resulting in groundwater-dominated hydrological processes. Numerous studies have highlighted the island's heterogeneous
aquifer structure, characterized by multi-layered perched and confined aquifers that respond sensitively to seasonal
precipitation inputs (Hahn et al., 1997; Koh et al., 2012; Kim et al., 2026). These hydrogeological conditions make isotopic
tracers particularly effective for identifying recharge elevations, estimating groundwater residence times, and interpreting
mixing processes between fresh and saline waters. Consequently, Jeju Island represents an ideal setting for developing spatially
85 resolved precipitation isotope datasets that aid groundwater modeling and ecohydrological investigations.

Climatically, Jeju Island lies in a transitional zone between temperate continental and subtropical maritime regimes. Its
climate is strongly shaped by monsoon circulation, seasonal shifts in moisture sources, and interactions between the Siberian
High and the North Pacific High. Winters (November to April) are influenced by cold, dry continental air masses, while
summers (June–September) are dominated by humid maritime tropical air advected from the Pacific Ocean. The average
90 annual temperature ranges from -3.4°C in winter to 27.9°C in summer, with a mean of 12.7°C . Annual precipitation exceeds
1,600 mm in most regions, with over half occurring during the summer monsoon period. These synoptic-scale seasonal
contrasts exert strong control on isotopic depletion and enrichment, contributing to well-defined seasonal patterns in $\delta^{18}\text{O}$, δD ,
and d-excess values (Lee et al., 2013). The combined influence of steep altitudinal gradients, varied moisture source trajectories,
and distinct monsoon circulation patterns creates complex spatial and temporal isotope dynamics that cannot be captured using
95 single-station monitoring approaches. Coastal regions are predominantly influenced by marine vapor and convective rainfall,



while higher elevations experience enhanced isotopic depletion due to progressive condensation and orographic precipitation. These conditions make Jeju Island an ideal natural laboratory to investigate altitude effects, moisture source variability, and monsoon-driven isotope seasonality using multi-site and long-term monitoring. Consequently, the spatial distribution of our 15 monitoring stations was intentionally designed to capture these gradients, extending from 10 m to over 1,500 m in elevation, covering both windward and leeward slopes, and spanning inland vs. coastal transitions.

2.2 Previous isotopic studies at Jeju island

Previous studies on Jeju Island have examined the stable isotope compositions of precipitation, groundwater, and cave water to characterize hydrological processes, moisture sources, and groundwater recharge mechanisms. Early work primarily focused on short-term observations from limited locations, often covering only single-site measurements or event-based sampling (Lee et al., 1999; Lee et al., 2003; Woo et al., 2013). These studies contributed valuable insights into seasonal isotope variability and moisture source influences but lacked spatial coverage, particularly across different elevation zones, windward–leeward slopes, and coastal vs. inland transitions. As a result, the isotopic gradients associated with topography, monsoon circulation, and localized convective processes remained largely unconstrained across the island. Consequently, there has been a critical need for a long-term, spatially resolved precipitation isotope dataset that simultaneously captures both temporal variability and island-wide spatial gradients, to improve hydroclimatic modeling and proxy calibration efforts.

Subsequent research expanded to include the isotopic characterization of groundwater, cave dripwater, and speleothems, demonstrating that modern precipitation isotope data are essential for calibrating paleoclimate proxies in Jeju’s volcanic landscapes (Woo et al., 2008; Jo et al., 2014). These studies identified that groundwater recharge is predominantly derived from high-elevation winter precipitation, while speleothem isotopic signals preserve a mixture of seasonal infiltration and moisture source variability (Lee et al., 2007; Kim et al., 2003). However, these investigations largely relied on extrapolated isotope lapse rates or interpolated GNIP data due to the absence of a spatially resolved precipitation isotope dataset collected simultaneously across multiple elevations and climatic regimes. This limitation has hindered the ability to accurately quantify spatial heterogeneity in isotopic elevation relationships, moisture source transitions, and monsoon driven fractionation processes, thereby constraining the development of reliable isoscapes and robust paleoclimate interpretations for Jeju Island (Peng et al., 2010; Ha et al., 2013).

More recent studies employed isotope-enabled models and atmospheric satellite observations to analyze moisture source trajectories and synoptic-scale vapor dynamics affecting Jeju Island (Yoshimura et al., 2011; Lee et al., 2013). These works highlighted the importance of monsoon-driven isotopic inversion (summer-depleted / winter-enriched), but validation of these model outputs was limited due to sparse in situ observations and the lack of a high-density monitoring network. The previous studies could therefore characterize either temporal changes or spatial differences, but not both concurrently. No prior study has produced a multi-year, multi-site dataset capturing both spatial and temporal variability of precipitation isotopes



across volcanic terrain, which is essential for quantifying altitude effects, seasonal moisture source changes, monsoon circulation patterns, and Rayleigh distillation across elevation gradients.

130 The present dataset fills this critical gap by providing simultaneous spatial and temporal precipitation isotope observations from 15 stations over a continuous 39-month period. It enables, for the first time on Jeju Island, quantitative assessment of both seasonal isotope cycles and altitude-dependent depletion patterns, facilitating more accurate characterization of recharge dynamics, topographic gradients, and paleoenvironmental interpretations. The dataset also offers a robust observational basis for calibrating isotope-enabled climate models and for developing regional isoscape frameworks.

2.3 Sampling and analytical methods

135 Precipitation samples were collected continuously from September 2000 to December 2003 at 15 strategically selected stations distributed across Jeju Island (10–1,500 m a.s.l.), covering distinct topographic, climatic, and geographic features (Figure 1). The sampling network was designed to represent windward and leeward slopes, coastal-to-inland transitions, and altitudinal gradients, allowing simultaneous observation of spatial and temporal isotope variability. Stations were classified into four elevation zones (coastal <100 m, lowland 100–300 m, mid-elevation 300–800 m, and high-elevation >800 m) to
140 quantify altitude effects and orographic precipitation processes.

In total, 462 precipitation samples were analyzed for $\delta^{18}\text{O}$, δD , and d-excess. Analyses were conducted using an Isoprime isotope ratio mass spectrometer (IRMS) at the Korea Basic Science Institute (KBSI), following IAEA protocols. $\delta^{18}\text{O}$ measurements were performed using $\text{CO}_2\text{-H}_2\text{O}$ equilibration and cryogenic condensation, whereas δD was analyzed by chromium reduction (Cr-Pyrolysis) to generate H_2 gas. Analytical precision was $\pm 1.0\text{‰}$ for δD and $\pm 0.1\text{‰}$ for $\delta^{18}\text{O}$, based
145 on repeated internal standards calibrated against VSMOW2, SLAP2, and GISP reference waters. All reported values follow the conventional δ -notation relative to VSMOW:

$$\delta = \left(\frac{R_x}{R_{\text{VSMOW}}} - 1 \right) \times 1000$$

where R_x is the ratio of heavy to light isotopes ($^{18}\text{O}/^{16}\text{O}$ or D/H) in the sample.

150 Quality control and quality assurance included duplicate analysis of 10% of samples, drift correction using internal laboratory standards, and exclusion of samples suspected of sub-cloud evaporation (based on anomalously high δ -values or low d-excess). Data screening criteria included excessive exposure time, leakage, and incomplete rainfall events. Meteorological data (temperature, monthly precipitation amount, relative humidity) from nearby national weather stations



(Korea Meteorological Administration) were used to complement isotope observations. These metadata enable combined
155 interpretation of isotope variability in relation to rainfall intensity, moisture source changes, and seasonality.

3 Results

3.1 Temporal variations of precipitation isotopes

The isotopic compositions of precipitation on Jeju Island exhibited pronounced seasonal variabilities during the 39-month
monitoring period (September 2000 to December 2003), reflecting changes in atmospheric circulation, moisture origin,
160 temperature, and monsoon precipitation regimes. The $\delta^{18}\text{O}$ and δD values ranged from -13.20‰ to -2.02‰ and -93.35‰ to
 -5.82‰ , respectively, across all stations and sampling periods. The d-excess ($d = \delta\text{D} - 8 \times \delta^{18}\text{O}$) values ranged from -2.4‰
to 23.1‰ , with notably higher values during winter, indicating stronger kinetic fractionation and lower humidity at the
moisture source, whereas summer values reflected humid maritime air masses. Monthly averaged values revealed a
consistent seasonal pattern characterized by isotopic depletion during summer (between June and September) and
165 enrichment during winter (between November and February), aligning with the East Asian monsoon-driven inversion pattern
previously reported for coastal and island regions (Lee et al., 2003; Uemura et al., 2012). Unlike continental mid-latitude
regions, where heavy isotopes are typically enriched in warm months, Jeju Island demonstrated depleted summer isotopic
values due to large-scale convective rainfall, enhanced rainout, and strong maritime moisture influence. These seasonal
behaviors were further supported by correlation analysis, which showed that d-excess exhibited the strongest inverse
170 relationship with air temperature ($R^2 = 0.77$, $p < 0.0001$) compared to $\delta^{18}\text{O}$ ($R^2 = 0.07$) and δD ($R^2 = 0.29$), confirming its
higher sensitivity to moisture source humidity and evaporation conditions (Table 1).

The isotopic time-series exhibit distinct seasonal extrema, with minimum $\delta^{18}\text{O}$ and δD values occurring between August
and September and maximum values observed from January to February (Figure 2). This pattern indicates that precipitation
during the peak summer monsoon carries the most isotopically depleted signatures, reflecting intensified convective activity,
175 long-distance moisture transport, and enhanced Rayleigh distillation associated with summer precipitation. In contrast, isotopic
enrichment during winter precipitation is likely related to lower atmospheric humidity, stronger sub-cloud evaporation, and
increased contributions from drier continental air masses during the cold season (Tao et al., 2025). Unlike $\delta^{18}\text{O}$ and δD , the
secondary isotope parameter d-excess shows a more complex seasonal evolution, characterized by a quadratic rather than
sinusoidal pattern, indicating a stronger sensitivity to kinetic fractionation processes (Dansgaard, 1964). Monthly d-excess
180 values are lowest during summer months, consistent with highly humid maritime moisture sources, whereas significantly
higher winter values suggest reduced humidity, enhanced evaporative enrichment at moisture source regions, and stronger
continental influences. Correlation analysis further supports this interpretation, demonstrating that d-excess is more strongly
related to air temperature ($R^2 = 0.77$, $p < 0.001$) than to precipitation amount ($R^2 = 0.52$, $p < 0.001$), indicating that seasonal



185 changes in moisture source humidity and evaporation conditions exert a stronger control than rainfall intensity alone (Guo et al., 2021).

Seasonal analysis of the local meteoric water lines (LMWLs) further reveals systematic variations in $\delta^{18}\text{O}$ vs $\delta^2\text{H}$ relationships associated with changes in atmospheric circulation and moisture source conditions over Jeju Island (Figure 3; Table 2). The annual LMWL derived from the full dataset ($\delta^2\text{H} = 8.17 \times \delta^{18}\text{O} + 15.72$, $R^2 = 0.89$) reflects the integrated influence of both summer monsoon and winter precipitation regimes, but seasonal regressions demonstrate clear contrasts
190 between warm and cold seasons (Fritz et al., 2022). During the summer monsoon period (JJAS), the LMWL exhibits a relatively higher slope and a markedly lower intercept, consistent with precipitation dominated by humid maritime moisture sources and extensive rainout under convective conditions, which suppresses kinetic fractionation during evaporation. In contrast, the winter LMWL (NDJF) is characterized by a reduced slope and an elevated intercept, indicating enhanced kinetic effects associated with lower humidity, stronger evaporation at the moisture source, and increased contributions from
195 continental air masses transported over the Yellow Sea. Transitional seasons display intermediate LMWL characteristics, reflecting the gradual shift between these two dominant circulation regimes. These seasonal differences in LMWL geometry are consistent with the observed seasonal behavior of d-excess and corroborate the interpretation that moisture source humidity and atmospheric transport pathways exert a first-order control on isotope relationships in precipitation. The well-resolved seasonal LMWLs presented here provide a robust reference framework for interpreting groundwater recharge processes, cave
200 dripwater isotopes, and paleoclimate archives in monsoon-influenced volcanic island environments, where mixing of seasonal signals can otherwise obscure the climatic interpretation of isotope records.

3.2 Spatial variations of precipitation isotopes

The spatial distribution of precipitation isotopes across Jeju Island demonstrates strong topographic control, primarily driven by orographic uplift, Rayleigh distillation, and varying exposure to maritime air masses. As shown in Figure 4, $\delta^{18}\text{O}$ and δD
205 values exhibit progressive depletion with increasing elevation, forming a distinct altitudinal gradient characteristic of mountainous volcanic terrains. Based on 462 precipitation samples across 15 stations, $\delta^{18}\text{O}$ decreased at an average rate of -1.5‰ per 1000 m, with a strong linear fit ($R^2 = 0.88$, $p < 0.005$), while δD showed a corresponding trend of -11‰ per 1000 m ($R^2 = 0.77$). These lapse rates are broadly consistent with those reported for other high-relief island environments in East Asia and the western Pacific, confirming the influence of orographic fractionation on isotopic depletion.

210 While $\delta^{18}\text{O}$ and δD showed clear elevation-driven depletion trends, d-excess displayed weaker spatial dependence, with only modest changes across elevation groups ($R^2 = 0.39$). Higher d-excess values at mid- and high-altitude locations indicate potential influence of drier continental air masses and moisture recycling during winter months, while lower values in coastal stations reflect more humid maritime moisture and stronger kinetic fractionation at the ocean–atmosphere interface. The combined analysis of $\delta^{18}\text{O}$, δD , and d-excess suggests that spatial variability in precipitation isotopes on Jeju



215 Island is shaped not only by orographic lifting but also by seasonal shifts in moisture sources and varying humidity
conditions during condensation and transport. The spatially resolved dataset presented here is the first to quantify the
simultaneous effects of altitude, topographic orientation, and monsoon circulation on precipitation isotopes across Jeju
Island. These results provide a robust observational basis for estimating groundwater recharge elevations, refining local
isotope models, and improving isotope-enabled hydrological simulations in volcanic island settings. Furthermore, the
220 observed spatial gradients serve as critical calibration inputs for interpreting isotopic signals preserved in speleothems, cave
dripwater, and other paleoclimate archives, contributing to improved proxy-based climate reconstructions in East Asia.

4 Discussion

4.1 Temporal variations of precipitation isotopes

The long-term monitoring across Jeju Island provides one of the few datasets in East Asia that captures both the amplitude and
225 phase of seasonal isotopic cycles, allowing for robust quantification of seasonal offsets in $\delta^{18}\text{O}$, δD , and d-excess. Unlike short-
duration event-based sampling campaigns or single-site monitoring records, this dataset enables assessment of multi-year
seasonal stability, which is essential for calibrating isotope-enabled climate models, such as IsoGSM and iCESM, and for
validating isotopic proxies preserved in groundwater and speleothem archives (Yoshimura et al., 2011; Brady et al., 2019).
The consistent occurrence of isotopic minima during summer (June to September) and maxima during winter (November to
230 February) supports its application in seasonal weighting of recharge, particularly in volcanic aquifers where infiltration timing
determines groundwater residence and isotope signatures.

The use of fitted sinusoidal curves to represent monthly mean $\delta^{18}\text{O}$ and δD values enhances the dataset's usability for
both modeling and proxy calibration (Figure 5). Unlike conventional raw isotopic time-series, the seasonal cycle parameters
(baseline, amplitude, and phase) extracted from the periodic fitting approach allow direct input into hydrological and land-
235 surface models that require temporally smoothed isotope forcing data (Nelson et al., 2021). This is particularly valuable in
monsoon climates, where conventional amount-weighted averages do not capture seasonal variability in moisture source or
atmospheric circulation. The documented seasonal cycle also defines a reference framework for distinguishing between
temperature-based fractionation (winter enrichment) and moisture-source depletion (summer monsoon rainout), facilitating
attribution of isotope variation to underlying atmospheric processes rather than simple temperature effects. The secondary
240 isotopic parameter, d-excess, however, exhibited a more complex seasonal pattern, deviating from pure sinusoidal behavior.
Its strong inverse relationship with temperature and relative humidity confirms that d-excess can serve as an effective
indicator of moisture source humidity, ocean-atmosphere evaporation conditions, and sub-cloud kinetic fractionation during
transport (Schoenemann et al., 2016). This sensitivity makes d-excess particularly valuable for identifying shifts between
continental (high d-excess) and maritime (low d-excess) moisture sources, especially during winter and summer seasons,
245 respectively. When integrated with satellite water vapor isotope datasets (e.g., TES, TROPOMI) or isotope-enabled



reanalysis, the dataset can help improve representations of monsoon moisture recycling, boundary layer humidity, and airmass trajectory modeling (Worden et al., 2007).

250 Combined, the seasonal dynamics observed in $\delta^{18}\text{O}$, δD , and d-excess across Jeju Island demonstrate that precipitation isotopes are shaped not only by local climate conditions but also by large-scale atmospheric circulation patterns, including the East Asian monsoon, Siberian High, and Pacific moisture transport. The magnitude and consistency of seasonal variations across three years indicate that the dataset is suitable for developing monthly climatological isotope normals, which can be used to support long-term groundwater recharge analysis, paleoclimate calibration, and isotope-based hydroclimate reconstruction in monsoon-affected regions.

4.2 Spatial (altitudinal) variations of precipitation isotopes

255 Over the past decade, a wide range of methodologies, encompassing spatial interpolation, numerical modeling, and emerging artificial intelligence approaches, have been applied to elucidate the spatial distribution of precipitation isotopes (Hassanzadeh et al., 2023). In volcanic island settings, the most prominent driver of isotopic heterogeneity is the “altitude effect,” wherein both $\delta^{18}\text{O}$ and $\delta^2\text{H}$ values exhibit systematic depletion with increasing elevation. This phenomenon reflects the interplay of orographic uplift, temperature lapse rates, and Rayleigh distillation, all of which act to progressively remove heavier isotopes
260 from ascending air masses. Consequently, altitude-dependent fractionation provides a quantitative foundation for modeling how isotopic signals vary across different topographic zones. Such insights are critical not only for understanding local climate hydrology feedbacks but also for refining paleoclimate proxies. For instance, speleothem records incorporate the isotopic signatures of infiltrating water, which can be more accurately interpreted when the relationship between precipitation isotopes and altitude is well-constrained. Furthermore, this altitude-based framework has proven instrumental in estimating recharge
265 elevations, as it allows researchers to infer the approximate altitude at which groundwater was originally deposited, thereby shedding light on aquifer heterogeneity and replenishment mechanisms.

To further characterize spatial heterogeneity, the monitoring stations were grouped by cardinal direction (north, south, east, and west), allowing comparison of elevation-dependent isotope patterns under differing marine influences, prevailing wind regimes, and topographic shielding (Figure 6). Across all stations, precipitation isotopes exhibit a clear altitude effect,
270 with mean lapse rates of -0.15‰ per 100 m for $\delta^{18}\text{O}$ and -1.09‰ per 100 m for δD (Table 3). Directional analyses reveal systematic differences in the strength of this elevation dependence. The strongest isotopic depletion with altitude is observed on the northern and western slopes, where $\delta^{18}\text{O}$ lapse rates reach -0.18‰ and -0.14‰ per 100 m, respectively, accompanied by correspondingly steeper δD gradients. These regions are more frequently influenced by winter continental air masses and enhanced upslope lifting, conditions that favor progressive rainout and stronger isotopic depletion. In contrast, stations on
275 the southern side of the island show a weaker elevation dependence for both $\delta^{18}\text{O}$ and δD ($\delta^{18}\text{O}$: -0.085‰ per 100 m, $R^2 = 0.59$), consistent with stronger maritime influence and reduced condensation efficiency associated with proximity to the open



ocean. Together, these directional contrasts indicate that spatial variability in precipitation isotopes across Jeju Island is governed not only by elevation but also by the combined effects of prevailing wind direction and windward–leeward positioning in a volcanic island setting.

280 Our dataset from fifteen sampling stations across Jeju Island (Figure 6) confirms a robust negative correlation between precipitation isotopes and station altitude. Specifically, the relationship

$$\delta^{18}\text{O} = -0.0015 \times Alt \pm 0.016 \quad (R^2=0.88, p < 0.005), \quad (1)$$

where *Alt* is the altitude (m). It indicates that $\delta^{18}\text{O}$ decreases by approximately 0.15‰ per 100 m increase in elevation. As summarized in Table 3 for each cardinal direction, the coefficient of determination (R^2) and *p*-value statistics suggest that this
285 altitudinal dependence effectively explains much of the observed spatial variability, except for some outliers in the southern region where additional factors, such as maritime influences or localized weather patterns, may dominate. These findings corroborate the broader principle that steep orographic gradients can significantly alter local isotopic compositions, emphasizing the need to integrate topographic effects when interpreting precipitation isotope data (Wang et al., 2024).
290 Moreover, recognizing the magnitude of this lapse rate helps refine hydrogeological models by enabling more accurate estimates of how precipitation recharges various aquifer systems, especially in regions where groundwater constitutes the primary water supply.

Examining altitudinal gradients along multiple cardinal directions provides further clarity on the spatial complexity of isotope fractionation across Jeju. This multidirectional perspective disentangles purely altitude-driven depletions from other spatial influences, such as the proximity to marine air masses or the prevailing wind trajectories. By constructing isotopic
295 transects from north, south, east, and west, it becomes possible to pinpoint anisotropic depletion patterns and better discern localized controls on isotopic variability. These data, in turn, enhance the spatial resolution of isotope-based models and strengthen our capacity to predict recharge elevations and groundwater flow paths. The ability to distinguish between low-elevation recharge derived from coastal precipitation and high-elevation recharge sourced from more depleted rainfall is especially valuable for managing volcanic island aquifers, which often exhibit complex stratigraphy and vulnerability to
300 contamination. Ultimately, integrating cardinal-direction transects with altitude effect analyses offers a comprehensive approach to understanding both the spatial and altitudinal dimensions of precipitation isotope variability, supporting improved water resource management and more nuanced paleoclimate reconstructions.

4.3 Isotope enabled general circulation model (GCM)

A comparison between a general circulation model that enables isotopic variations and actual observational data conducted.
305 We used IsoGSM, which is a global atmospheric model incorporating stable water isotope fractionation processes into a general circulation model (GCM), enabling the simulation and analysis of isotopic variations in atmospheric and hydrological processes (Yoshimura et al., 2011). In this study, we evaluate the performance of this model by comparing IsoGSM outputs



with observational data. The IsoGSM provides monthly mean isotope data, and for this study, we analyzed the precipitation isotope compositions over Jeju Island using three grid cells that recorded precipitation rates exceeding 0.2 mm/day. Monthly mean values and standard deviations were computed for each grid cell, and the range of ± 1 standard deviation was used to construct a banded representation encompassing all three grid cells (Figure 7). Observed isotope values were also calculated as monthly means.

The comparison reveals that the IsoGSM simulations closely replicate the observed $\delta^{18}\text{O}$ and δD values during MAJJAS (May–October), whereas ONDJF (November–April) simulations exhibit a systematic overestimation of isotopic enrichment. This discrepancy is also reflected in the secondary parameter, d-excess, suggesting systematic biases in winter precipitation isotopic composition. The overestimation of $\delta^{18}\text{O}$ and δD in winter may be attributed to limitations in IsoGSM’s representation of mesoscale convective systems and water vapor transport mechanisms. Winter precipitation over Jeju Island is strongly influenced by cold Siberian air masses moving over the warm Yellow Sea, inducing significant heat and moisture fluxes that enhance convective snow formation (Lee et al., 2003). However, IsoGSM may struggle to capture the enhancement of snowfall due to the sea surface heat flux and convective instability. Additionally, as convective snowstorms frequently occur over Jeju Island due to localized convergence and topographic effects, the model’s relatively coarse resolution may fail to adequately represent such small-scale convective events. Previous studies have shown that winter precipitation in Jeju is modulated by synoptic-scale atmospheric circulations and moisture recycling from the Yellow Sea and East China Sea, which significantly influence isotope fractionation processes (Lee et al., 2003). The inability of IsoGSM to fully resolve these processes likely contributes to the observed overestimation. Conversely, summer precipitation is primarily governed by large-scale processes such as the Meiyu–Baiu frontal system, which is driven by the pressure gradient between the North Pacific High and the Siberian High. These systems facilitate a sustained influx of moisture from the southwest, leading to extensive precipitation over Jeju Island (Lee et al., 2003). As IsoGSM effectively captures large-scale circulation and associated moisture transport, its simulations align well with observed isotope variations in summer. The relatively stable water vapor source and dominant large-scale control mechanisms likely contribute to the improved performance of the model during this season. These findings highlight the strengths and limitations of IsoGSM in reproducing stable isotope variations in precipitation. While the model effectively captures isotopic variations associated with large-scale systems, regional-scale processes such as sea-induced convection and localized convective snowfall require improved representation for more accurate isotope simulations in winter precipitation. Future work should focus on refining model physics, including the parameterization of sea–air interactions and mesoscale convective processes, to enhance the fidelity of isotope-enabled simulations in midlatitude regions.

4.4 Implications of characteristics of precipitation isotopes on paleoclimate study

We anticipate that this approach with dataset will be a useful tool for other overlapping disciplines including ecohydrology, alpine hydrology and the ongoing documentation of global water-cycle partitioning and dynamics. In addition, the characteristics of isotopic variations from precipitation can aid in a better understanding of the importance of the oxygen



340 isotope record in the paleoclimate reconstruction in the island. The refined isotopic framework has significant implications for
paleoclimate research. The sine function fitting offers a robust means to parameterize seasonal signals, which are crucial for
calibrating isotopic proxies in natural archives, such as speleothems in this volcanic island. By integrating the altitude effect
into the isotope-enabled model, we can better reconstruct spatially resolved past climate conditions and assess variations in
moisture sources and atmospheric circulation patterns. This comprehensive framework facilitates more accurate calibration of
345 isotope-enabled models and supports robust assessments of moisture transport and water resource dynamics across complex
landscapes. This enhanced interpretation capacity is also invaluable for building more accurate paleoclimate reconstructions
in regions with complex orography and climate patterns in East Asia, including the volcanic island.

Beyond its paleoclimate applications, this study provides critical insights for both speleothem analysis and water
resource management. Speleothems, which record the isotopic signature of precipitation, can now be interpreted with greater
350 confidence by correlating their records with the well-characterized seasonal and altitudinal isotopic variations documented in
this work. Furthermore, understanding these isotopic dynamics aids in tracing hydrological processes, such as groundwater
recharge and surface water contributions, thereby informing sustainable water resources strategies. Together, these
methodological advancements offer a powerful framework for advancing both fundamental climate science and applied water
management in coastal and island environments over East Asia.

355 5. Data availability

The precipitation isotope dataset presented in this study is publicly available through the Geo Big Data Open Platform at
https://doi.org/10.22747/paper_data.20260219.42 (Lee et al., 2026). The dataset contains precipitation-weighted monthly
mean values of $\delta^{18}\text{O}$, $\delta^2\text{H}$, and d-excess measured at 15 observation sites across Jeju Island along an elevation gradient from
10 to 1500 m and covers the period from September 2000 to December 2003 (39 months).

360 6 Summary

This study presents the stable isotopic compositions ($\delta^{18}\text{O}$, δD , and d-excess) of precipitation over Jeju Island and documents
clear seasonal variability. Periodic seasonal oscillations in $\delta^{18}\text{O}$ and δD were represented using sine-function fitting, whereas
a quadratic function captured the non-linear seasonal pattern of d-excess. These fitted relationships highlight systematic
seasonal shifts in precipitation isotope composition linked to changes in temperature, moisture sources, and large-scale
365 atmospheric circulation.

Spatial variability in the precipitation isotopes is predominantly controlled by an altitude effect, whereby isotopic values
become progressively depleted with increasing elevation due to enhanced orographic precipitation and associated Rayleigh
distillation processes. Regression analyses across different cardinal directions demonstrated that, except for the southern region



where marine influences are stronger, the altitude effect robustly explains the observed isotopic variability. This altitude-
370 dependent framework also enables the estimation of groundwater recharge elevations and the interpretation of speleothem
records, thereby enhancing our understanding of regional hydrological processes.

Furthermore, the integration of isotope-enabled general circulation models (e.g., IsoGSM) with observational data
provides critical insights into the mechanisms driving isotopic variations. While model simulations closely replicate summer
isotopic patterns, discrepancies in winter underscore the challenges in capturing mesoscale convective processes and localized
375 sea-air interactions. Overall, this comprehensive approach advances our understanding of both temporal and spatial isotope
dynamics, with significant implications for paleoclimate reconstruction, groundwater resource management, and broader
hydrological studies in complex volcanic island environments.

Author contributions. This study was conceptualized by KL and DK. Data were collected and analyzed by WP, YB, SK, HJ,
CK and WS. The paper was written by YK and JL, with contributions from all authors.

380 **Competing interests.** The contact author has declared that none of the authors has any competing interests.

Acknowledgements. The authors thank Kei Yoshimura and Hayoung Bong for sharing their model data.

Financial support. This work was financially supported by a National Research Foundation of Korea
(NRF2022R1A2C3007047) and partially supported by a grant (C638100) from the Korea Basic Science Institute. Additional
support was partially provided by the Korea Environment Industry & Technology Institute through Aquatic Ecosystem
385 Conservation Research Program, funded by the Korean Ministry of Environment (RS-2024-00332851) and the Basic Research
Project (25-3411) of the Korea Institute of Geoscience and Mineral Resources (KIGAM), funded by the Ministry of Science
and ICT.

References

- Brady, E., Stevenson, S., Bailey, D., Liu, Z., Noone, D., Nusbaumer, J., Otto-Bliesner, B. L., Tabor, C., Tomas, R., Wong, T.,
390 Zhang, J., and Zhu, J.: The Connected Isotopic Water Cycle in the Community Earth System Model Version 1, *Journal of
Advances in Modeling Earth Systems*, 11, 2547–2566, <https://doi.org/10.1029/2019ms001663>, 2019.
- Craig, H.: Isotopic variations in meteoric waters, *Science*, 133, 1702–1703, <https://doi.org/10.1126/science.133.3465.1702>,
1961.
- Dansgaard, W.: Stable isotopes in precipitation, *Tellus*, 16, 436–468, <https://doi.org/10.1111/j.2153-3490.1964.tb00181.x>,
395 1964.



- Dee, S., Bailey, A., Conroy, J. L., Atwood, A., Stevenson, S., Nusbaumer, J., and Noone, D.: Water isotopes, climate variability, and the hydrological cycle: recent advances and new frontiers, *Environmental Research: Climate*, 2, <https://doi.org/10.1088/2752-5295/acbe1>, 2023.
- Feng, X., Faiia, A. M., and Posmentier, E. S.: Seasonality of isotopes in precipitation: A global perspective, *Journal of Geophysical Research: Atmospheres*, 114, <https://doi.org/10.1029/2008jd011279>, 2009.
- 400 Fritz, M., Wetterich, S., McAlister, J., and Meyer, H.: A new local meteoric water line for Inuvik (NT, Canada), *Earth System Science Data*, 14, 57–63, <https://doi.org/10.5194/essd-14-57-2022>, 2022.
- Guan, H., Simmons, C. T., and Love, A. J.: Orographic controls on rain water isotope distribution in the Mount Lofty Ranges of South Australia, *Journal of Hydrology*, 374, 255–264, <https://doi.org/10.1016/j.jhydrol.2009.06.018>, 2009.
- 405 Guo, X., Gong, X., Shi, J., Guo, J., Domínguez-Villar, D., Lin, Y., Wang, H., and Yuan, D.: Temporal variations and evaporation control effect of the stable isotope composition of precipitation in the subtropical monsoon climate region, Southwest China, *Journal of Hydrology*, 599, <https://doi.org/10.1016/j.jhydrol.2021.126278>, 2021.
- Ha, K., Yoon, Y. Y., Lee, K. Y., Cho, S. Y., and Ko, K. S.: Seasonal variation in the isotopic contents of precipitation in Korea, *Journal of Radioanalytical and Nuclear Chemistry*, 296, 389–395, <https://doi.org/10.1007/s10967-012-2077-3>, 2012.
- 410 Hahn, J., Lee, Y., Kim, N., Hahn, C., and Lee, S.: The groundwater resources and sustainable yield of Cheju volcanic island, Korea, *Environmental Geology*, 33, 43–53, 1997.
- Hassanzadeh, A., Valdivielso, S., Vazquez-Sune, E., Criollo, R., and Corbella, M.: An open source Python library for environmental isotopic modelling, *Sci Rep*, 13, 1895, <https://doi.org/10.1038/s41598-023-29073-2>, 2023.
- Jo, K. N., Woo, K. S., Yi, S., Yang, D. Y., Lim, H. S., Wang, Y., Cheng, H., and Edwards, R. L.: Mid-latitude interhemispheric hydrologic seesaw over the past 550,000 years, *Nature*, 508, 378–382, <https://doi.org/10.1038/nature13076>, 2014.
- 415 Johnson, K. R. and Ingram, B. L.: Spatial and temporal variability in the stable isotope systematics of modern precipitation in China: implications for paleoclimate reconstructions, *Earth and Planetary Science Letters*, 220, 365–377, [https://doi.org/10.1016/s0012-821x\(04\)00036-6](https://doi.org/10.1016/s0012-821x(04)00036-6), 2004.
- Jung, H., Ahn, J., Iwahana, G., and Lee, J.: Understanding water flowpaths and origins in an Arctic Alaskan basin: Implications for permafrost hydrology under global warming, *Advances in Climate Change Research*, 16, 361–372, <https://doi.org/10.1016/j.accre.2025.03.001>, 2025.
- 420 Kim, M.-C., Shin, W.-J., Koh, E.-H., Koh, C.-S., Kim, G.-E., and Lee, K.-S.: Stable isotope signatures of precipitation and implications for groundwater recharge on Jeju volcanic island, South Korea, *Journal of Hydrology: Regional Studies*, 64, <https://doi.org/10.1016/j.ejrh.2026.103141>, 2026.
- 425 Kim, Y., Lee, K. S., Koh, D. C., Lee, D. H., Lee, S. G., Park, W. B., Koh, G. W., and Woo, N. C.: Hydrogeochemical and isotopic evidence of groundwater salinization in a coastal aquifer: a case study in Jeju volcanic island, Korea, *Journal of Hydrology*, 270, 282–294, [https://doi.org/10.1016/S0022-1694\(02\)00307-4](https://doi.org/10.1016/S0022-1694(02)00307-4), 2003.



- Koh, D.-C., Ha, K., Lee, K.-S., Yoon, Y.-Y., and Ko, K.-S.: Flow paths and mixing properties of groundwater using hydrogeochemistry and environmental tracers in the southwestern area of Jeju volcanic island, *Journal of Hydrology*, 432–433, 61–74, <https://doi.org/10.1016/j.jhydrol.2012.02.030>, 2012.
- Koh, E. H., Lee, E., Lee, K. K., and Moon, D. C.: Integrated application of a Bayesian mixing model, numerical model, and environmental tracers to characterize groundwater recharge sources in a mountainous area, *Sci Total Environ*, 853, 158619, <https://doi.org/10.1016/j.scitotenv.2022.158619>, 2022.
- Konecky, B. L., McKay, N. P., Churakova, O. V., Comas-Bru, L., Dassié, E. P., DeLong, K. L., Falster, G. M., Fischer, M. J., Jones, M. D., Jonkers, L., Kaufman, D. S., Leduc, G., Managave, S. R., Martrat, B., Opel, T., Orsi, A. J., Partin, J. W., Sayani, H. R., Thomas, E. K., Thompson, D. M., Tyler, J. J., Abram, N. J., Atwood, A. R., Cartapanis, O., Conroy, J. L., Curran, M. A., Dee, S. G., Deininger, M., Divine, D. V., Kern, Z., Porter, T. J., Stevenson, S. L., and von Gunten, L.: The Iso2k database: a global compilation of paleo- $\delta^{18}\text{O}$ and $\delta^2\text{H}$ records to aid understanding of Common Era climate, *Earth System Science Data*, 12, 2261–2288, <https://doi.org/10.5194/essd-12-2261-2020>, 2020.
- Lee, J., Feng, X., Faiia, A. M., Posmentier, E. S., Kirchner, J. W., Osterhuber, R., and Taylor, S.: Isotopic evolution of a seasonal snowcover and its melt by isotopic exchange between liquid water and ice, *Chemical Geology*, 270, 126–134, <https://doi.org/10.1016/j.chemgeo.2009.11.011>, 2010.
- Lee, J., Worden, J., Koh, D.-C., Yoshimura, K., and Lee, J.-E.: A seasonality of δD of water vapor (850–500 hPa) observed from space over Jeju Island, Korea, *Geosciences Journal*, 17, 87–95, <https://doi.org/10.1007/s12303-013-0003-5>, 2013.
- Lee, K. S., Grundstein, A. J., Wenner, D. B., Choi, M. S., Woo, N. C., and Lee, D. H.: Climatic controls on the stable isotopic composition of precipitation in Northeast Asia, *Climate Research*, 23, 137–148, 2003.
- Lee, K.-S., Kim, J.-M., Lee, D.-R., Kim, Y., and Lee, D.: Analysis of water movement through an unsaturated soil zone in Jeju Island, Korea using stable oxygen and hydrogen isotopes, *Journal of Hydrology*, 345, 199–211, <https://doi.org/10.1016/j.jhydrol.2007.08.006>, 2007.
- Lee, K., Ko, D., Kim, H., Park, Y., Kim, S., Jeong, H., Moon, W., Shin, J., Kim, H., and Lee, J.: *Water stable isotope data of precipitation in Jeju Island*, Geo Big Data Open Platform, https://doi.org/10.22747/paper_data.20260219.42, 2026.
- Lee, S., Shimada, J., and Kayane, I.: Stable isotopes in precipitation in the volcanic island of Cheju, Korea, *Hydrological Processes*, 13, 113–121, [https://doi.org/10.1002/\(sici\)1099-1085\(199901\)13:1<113::Aid-hyp698>3.0.Co;2-p](https://doi.org/10.1002/(sici)1099-1085(199901)13:1<113::Aid-hyp698>3.0.Co;2-p), 1999.
- Nelson, D. B., Basler, D., and Kahmen, A.: Precipitation isotope time series predictions from machine learning applied in Europe, *Proc Natl Acad Sci U S A*, 118, <https://doi.org/10.1073/pnas.2024107118>, 2021.
- Peng, T.-R., Wang, C.-H., Huang, C.-C., Fei, L.-Y., Chen, C.-T. A., and Hwong, J.-L.: Stable isotopic characteristic of Taiwan's precipitation: A case study of western Pacific monsoon region, *Earth and Planetary Science Letters*, 289, 357–366, <https://doi.org/10.1016/j.epsl.2009.11.024>, 2010.
- Posmentier, E. S., Feng, X., and Zhao, M.: Seasonal variations of precipitation $\delta^{18}\text{O}$ in eastern Asia, *Journal of Geophysical Research: Atmospheres*, 109, <https://doi.org/10.1029/2004jd004510>, 2004.



- Prada, S., Cruz, J. V., and Figueira, C.: Using stable isotopes to characterize groundwater recharge sources in the volcanic island of Madeira, Portugal, *Journal of Hydrology*, 536, 409–425, <https://doi.org/10.1016/j.jhydrol.2016.03.009>, 2016.
- Schoenemann, S. W. and Steig, E. J.: Seasonal and spatial variations of ^{17}O excess and $\delta^{18}\text{O}$ excess in Antarctic precipitation: Insights from an intermediate complexity isotope model, *Journal of Geophysical Research: Atmospheres*, 121, 465–475, <https://doi.org/10.1002/2016jd025117>, 2016.
- Tao, S., Xu, J., Xia, J., and Xiao, Y.: Influence of Sub-Cloud Evaporation on Precipitation Isotopes: Insights From Hourly-Scale Meteorological Assessment in a Large Lake in the East Asian Monsoon Region, *Hydrological Processes*, 39, <https://doi.org/10.1002/hyp.70152>, 2025.
- Uemura, R., Masson-Delmotte, V., Jouzel, J., Landais, A., Motoyama, H., and Stenni, B.: Ranges of moisture-source temperature estimated from Antarctic ice cores stable isotope records over glacial–interglacial cycles, *Climate of the Past*, 8, 1109–1125, <https://doi.org/10.5194/cp-8-1109-2012>, 2012.
- Wang, S., Wang, L., Yang, G., Xiao, Y., Argiriou, A. A., Shi, Y., Lei, S., and Zhang, M.: Altitude effect of precipitation isotopes in an arid mountain-basin system: Observation and modelling around the world’s second-largest shifting desert, *Journal of Hydrology*, 636, <https://doi.org/10.1016/j.jhydrol.2024.131351>, 2024.
- 475 Wang, S., Wang, S., Huang, X., Wang, H., Han, Y., Wang, S., and Qi, S.: Groundwater composition and stable isotopes as proxies to investigate paleoclimate change in permafrost thawing regions, *Applied Geochemistry*, 169, <https://doi.org/10.1016/j.apgeochem.2024.106036>, 2024.
- Woo, K. S., Jo, K. N., Yi, S. H., Yang, D. Y., and Li, H.-C.: Paleoclimatic investigation using oxygen isotope compositions of the YC-1 stalagmite, Yeongcheon Cave, Jeju Island, Korea for the past 600 years, *Journal of the Geological Society of Korea*, 49, 339–350, 2013.
- 480 Woo, K. S., Kim, J. C., Choi, D. W., Kim, J. K., Kim, R., and Nehza, O.: The origin of erratic calcite speleothems in the Dangcheomul Cave (lava tube cave), Jeju Island, Korea, *Quaternary International*, 176–177, 70–81, <https://doi.org/10.1016/j.quaint.2007.05.009>, 2008.
- Worden, J., Noone, D., Bowman, K., Tropospheric Emission Spectrometer Science, T., and Data, c.: Importance of rain evaporation and continental convection in the tropical water cycle, *Nature*, 445, 528–532, <https://doi.org/10.1038/nature05508>, 2007.
- 485 Xie, C., Zhao, L., Eastoe, C. J., Liu, X., Wang, N., Zhang, Z., Dong, X., and Liu, H.: Precipitation stable isotope composition, moisture sources, and controlling factors in Xi’an, Northwest China, *Atmospheric Research*, 280, <https://doi.org/10.1016/j.atmosres.2022.106428>, 2022.
- 490 Yoshimura, K., Frankenberg, C., Lee, J., Kanamitsu, M., Worden, J., and Röckmann, T.: Comparison of an isotopic atmospheric general circulation model with new quasi-global satellite measurements of water vapor isotopologues, *Journal of Geophysical Research*, 116, <https://doi.org/10.1029/2011jd016035>, 2011.



495 **Table 1.** Correlations between isotopic compositions of precipitation and meteorological parameters

	Air temperature			Precipitation amount		
	Slope	R^2	p	Slope	R^2	p
$\delta^{18}\text{O}$	-0.07	0.07	0.10	-0.0021	0.024	0.34
δD	-1.34	0.29	0.0003	-0.047	0.15	0.014
d-excess	-0.76	0.77	0.0001	-0.031	0.52	0.0001

R^2 and p denote the coefficient of determination and p -value, respectively



500 **Table 2.** Summary of previous studies defining the local meteoric water line (LMWL)

	Sampling duration	Locality in Jeju island	Relationships
S. Lee et al. (1999)	12 months	12 locations	All: $\delta D = 8.39 \times \delta^{18}O + 18.59$ ($n^a = 12$) All: $\delta D = (8.38 \pm 0.33) \times \delta^{18}O + (19.15 \pm 0.85)$ ($R^2 = 0.85$, $n = 109$)
Lee et al. (2003)	24 months	Seongsan	S (JJAS, $R^2 = 0.98$, $n = 43$) $\delta D = (7.94 \pm 0.20) \times \delta^{18}O + (8.87 \pm 1.46)$ W (NDJF, $R^2 = 0.98$, $n = 43$): $\delta D = (6.88 \pm 0.52) \times \delta^{18}O + (20.79 \pm 3.17)$
Lee et al. (2007)	12 months	a small research site	S (JJA, $R^2 = 0.999$, $n = 3$) $\delta D = 8.434 \times \delta^{18}O + 11.06$ W (NDJ, $R^2 = 0.999$, $n = 3$): $\delta D = 8.70 \times \delta^{18}O + 27.22$ S (JJA, $R^2 = 0.99$, $n = 27$) $\delta D = 7.73 \times \delta^{18}O + 4.82$
Ha et al. (2013)	12 months	9 locations	W (DJF, $R^2 = 0.83$, $n = 19$): $\delta D = 6.05 \times \delta^{18}O + 13.58$ All: $\delta D = (8.17 \pm 0.13) \times \delta^{18}O + (15.72 \pm 0.97)$ ($R^2 = 0.89$, $n = 462$, $p^b < 0.0001$)
Our study	39 months	15 locations	S (JJAS, $R^2 = 0.96$, $n = 156$) $\delta D = (7.91 \pm 0.13) \times \delta^{18}O + (8.02 \pm 1.10)$ W (NDJF, $R^2 = 0.98$, $n = 148$): $\delta D = (7.68 \pm 0.12) \times \delta^{18}O + (19.59 \pm 0.91)$

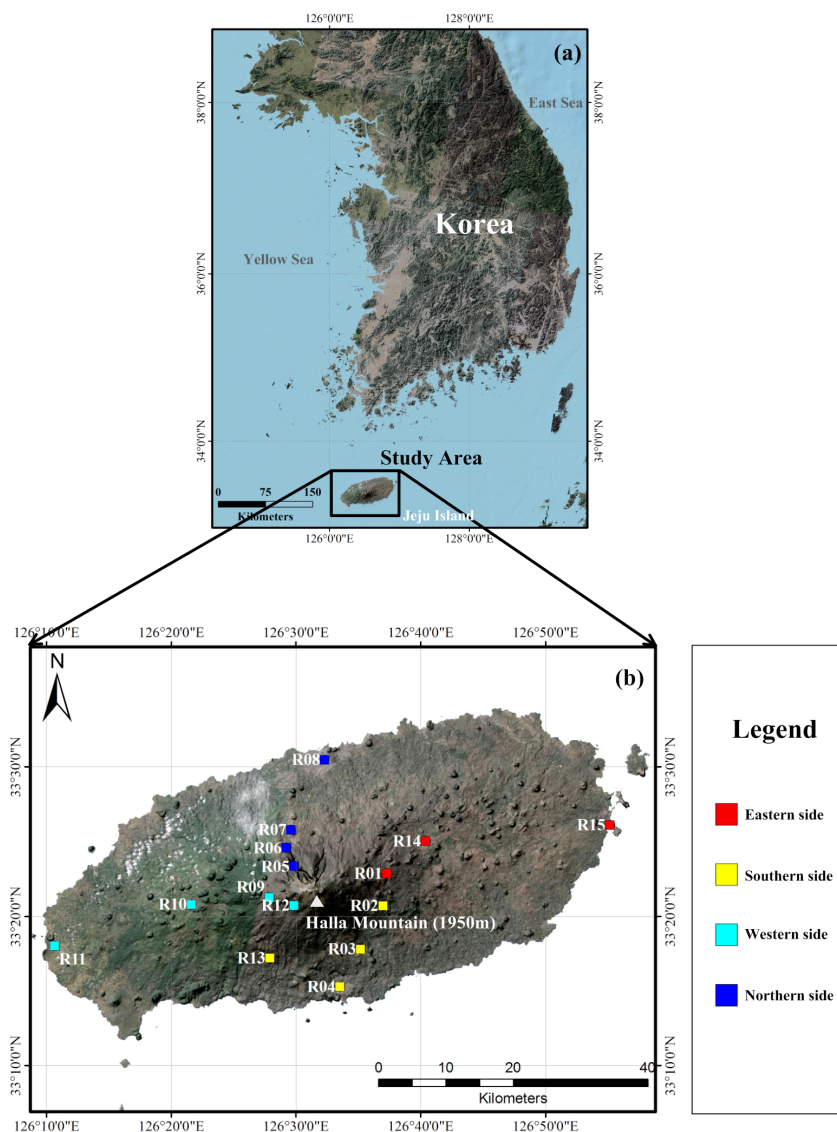
a: number of samples

b: probability



Table 3. Linear regression equations of precipitation isotopes and altitude for each cardinal direction

	Cardinal direction	Gradient (per 100 m)	R^2	p
$\delta^{18}\text{O}$	All	-0.15 ± 0.016	0.88	0.0001
	East	-0.14 ± 0.017	0.99	0.076
	West	-0.14 ± 0.014	0.98	0.01
	South	-0.085 ± 0.0051	0.59	0.23
	North	-0.18 ± 0.012	0.99	0.0042
δD	All	-1.09 ± 0.17	0.77	0.0001
	East	-0.86 ± 0.32	0.99	0.023
	West	-0.98 ± 0.14	0.96	0.020
	South	-1.38 ± 0.1	0.99	0.0055
	North	-1.38 ± 0.1	0.99	0.0055
d-excess	All	0.14 ± 0.048	0.39	0.014
	East	0.29 ± 0.17	0.75	0.34
	West	0.15 ± 0.028	0.93	0.036
	South	0.063 ± 0.0095	0.96	0.022
	North	0.063 ± 0.0095	0.96	0.022



515

Figure 1. Location of the fifteen precipitation sampling stations on Jeju volcanic island, South Korea. (a) Regional setting of Jeju Island relative to the Korean Peninsula. (b) Distribution of monitoring stations across the island, classified by cardinal direction (north, south, east, and west) and spanning elevations from approximately 10 to 1,500 m above sea level. The central volcanic edifice of Mt. Halla is indicated.

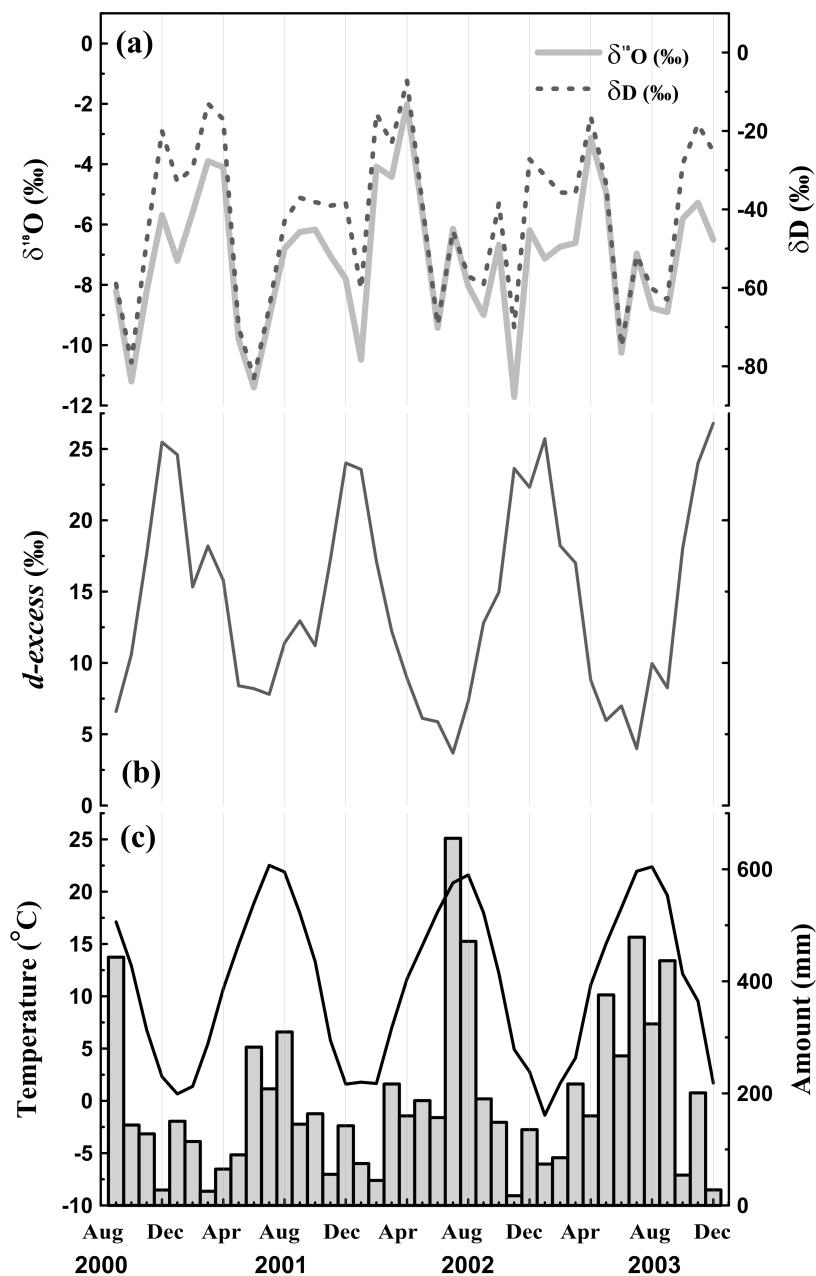
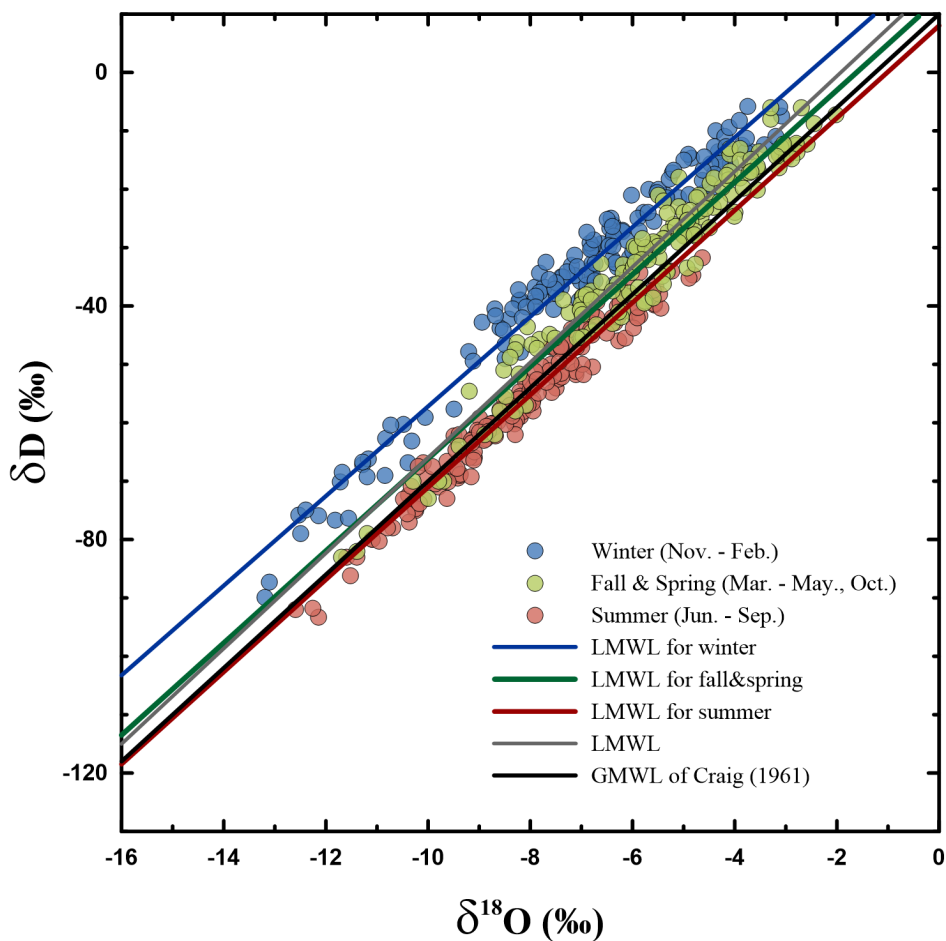
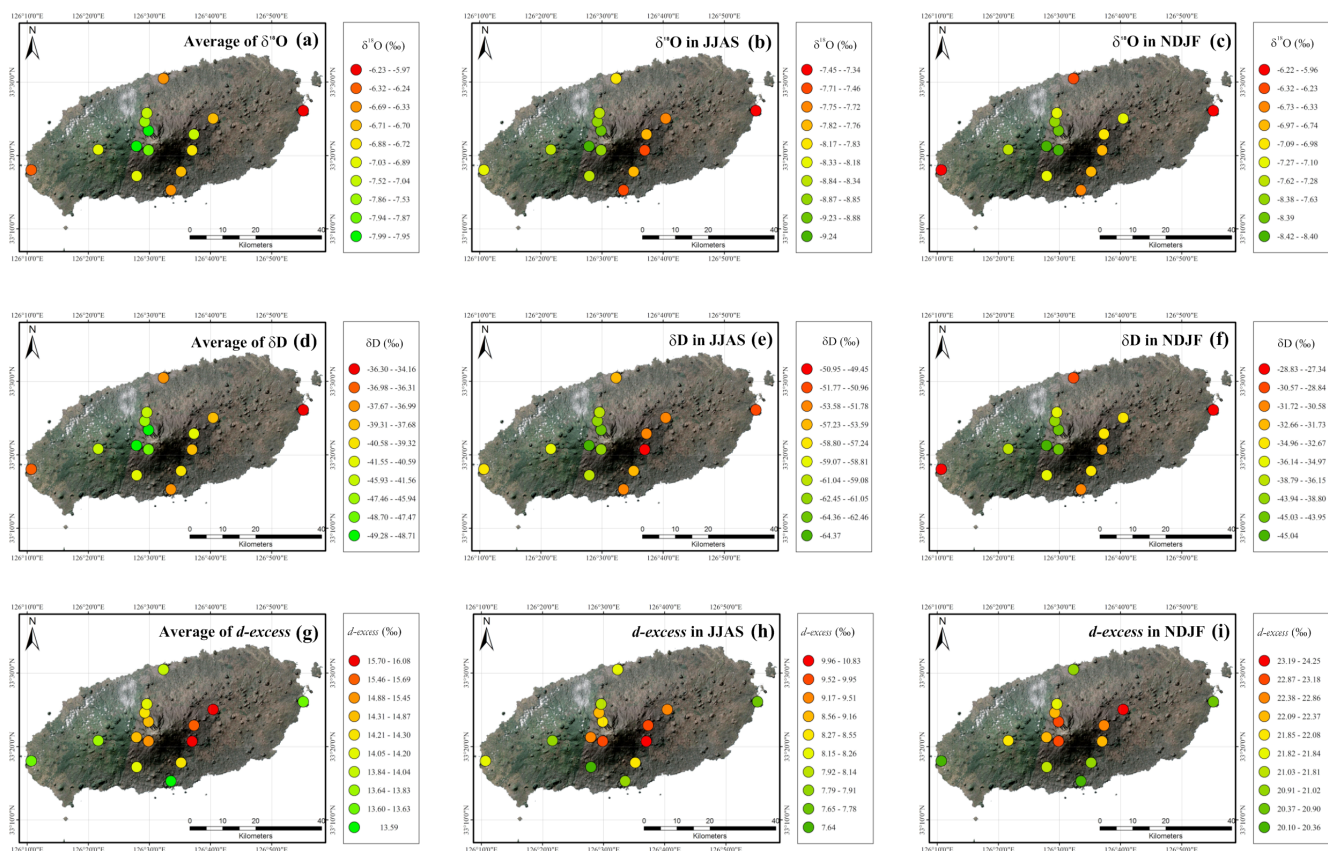


Figure 2. Temporal variations of monthly mean air temperature, precipitation amount, and stable isotopic compositions of precipitation ($\delta^{18}\text{O}$, δD , and d-excess) at Jeju Island from September 2000 to December 2003. Isotopic values are shown as monthly means aggregated across all stations.

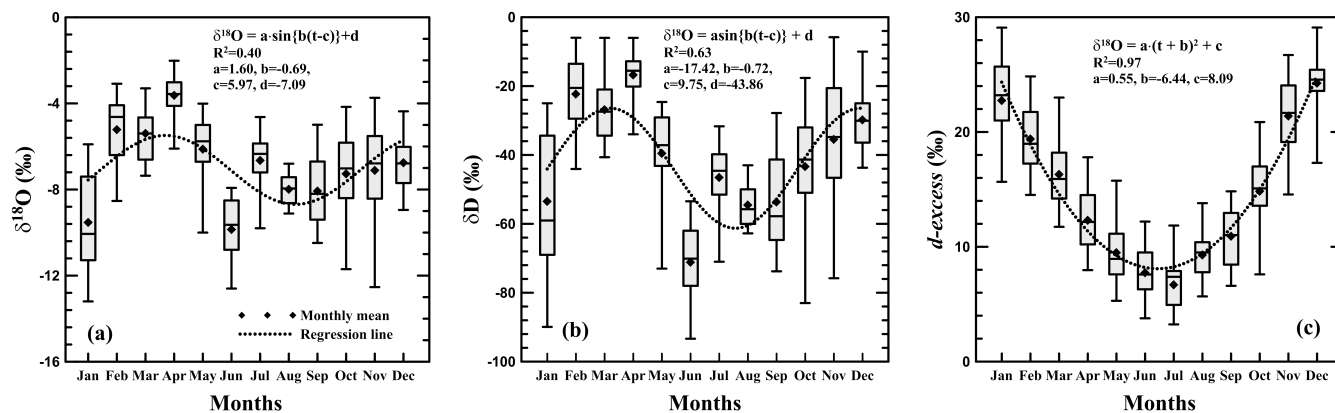
520



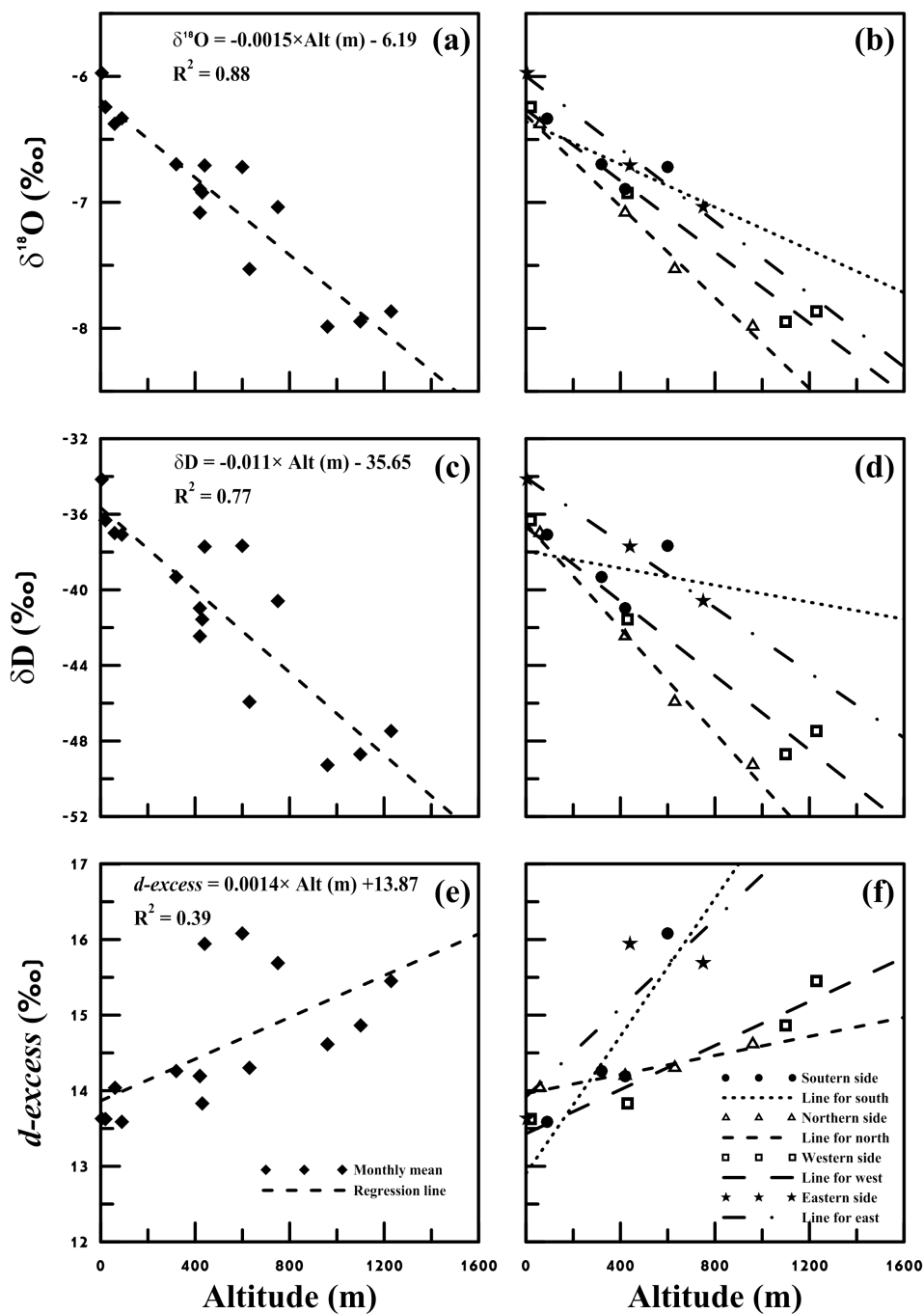
525 **Figure 3.** Local meteoric water lines (LMWLs) derived from precipitation isotope data, shown separately for summer (JJAS), winter (NDJF), and transitional seasons (spring and fall). Seasonal regression lines are compared with the global meteoric water line (GMWL; Craig, 1961). Data points represent individual precipitation samples.



530 **Figure 4. Spatial distribution of mean precipitation isotopic compositions across Jeju Island. Panels show island-wide patterns of $\delta^{18}\text{O}$, δD , and d -excess based on station-averaged values, as well as seasonal means for summer (JJAS) and winter (NDJF). Colors indicate isotopic magnitude, highlighting spatial gradients associated with elevation and proximity to the coast.**

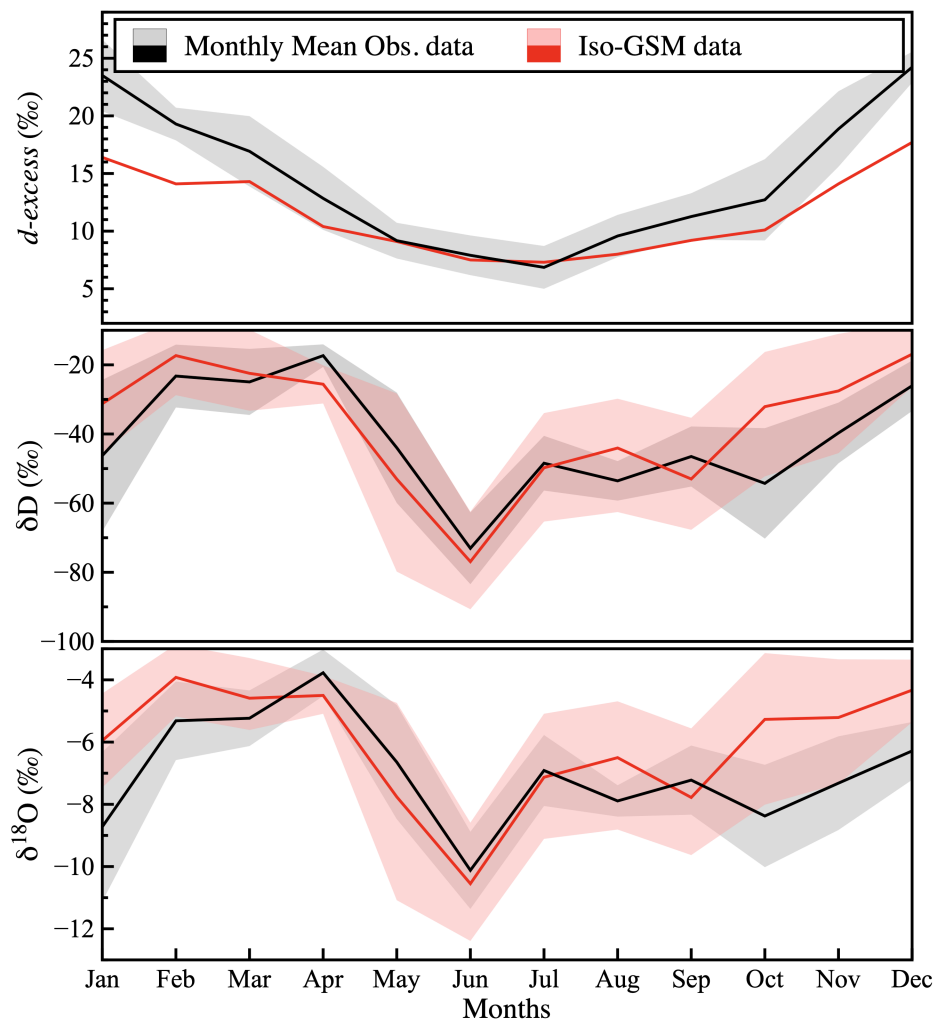


535 **Figure 5. Seasonal variations of precipitation isotopes fitted using sinusoidal and quadratic functions. Monthly mean values of (a) $\delta^{18}\text{O}$ and (b) δD are fitted with sinusoidal curves to characterize amplitude, phase, and baseline composition, while (c) $d\text{-excess}$ is fitted with a quadratic function to capture its non-linear seasonal behavior. Boxes represent interquartile ranges, and whiskers indicate minimum and maximum values.**



540

Figure 6. Altitude effects on precipitation isotope compositions across Jeju Island. Relationships between station elevation and monthly mean values of (a) $\delta^{18}\text{O}$, (c) δD , and (e) $d\text{-excess}$ are shown for all stations, together with linear regression lines. Panels (b), (d), and (f) illustrate directional differences in isotope–altitude relationships for north-, south-, east-, and west-facing slopes.



545

Figure 7. Comparison between observed monthly mean precipitation isotope compositions and simulations from the isotope-enabled general circulation model IsoGSM. Seasonal cycles of $\delta^{18}\text{O}$, δD , and $d\text{-excess}$ are shown, with shaded bands indicating ± 1 standard deviation of model outputs across relevant grid cells. Observed values are plotted as monthly means averaged over all stations.

550